RADIOTRONICS

Vol. 28, No. 7 July, 1963

IN THIS ISSUE

7

AN AWV PUBLICATION

REGISTERED IN AUSTRALIA FOR TRANSMISSION BY POST AS A PERIODICAL.

GALLIUM ARSENIDE VARACTOR DIODES

L. H. GIBBONS, Jr., A. E. WIDMER, and M. F. LAMORTE, Ldr.
Advanced Development, Semiconductor and Materials Division, Somerville, N.J.

This new small-area diffused-junction GaAs varactor diode has typical cutoff frequencies over 250 Gc, and is designed for low-noise parametric amplifiers. Circuit-performance gain, bandwidth, and noise figures are outstanding.

Semiconductor variable-capacitance diodes have become increasingly important in applications such as parametric amplification and subharmonic and harmonic frequency generation. Varactor diodes with satisfactory characteristics have been available for frequencies approaching the microwave region, but the absence of suitable diodes for higher frequencies has hampered efforts to seek out new (higher) frequency communication bands.

The small-area diffused-junction GaAs varactor diode described here is designed for use in low-noise parametric amplifiers. Results of application studies are also included because the data obtained were useful in achieving the optimum design of the diode.

VARACTOR-DIODE EQUIVALENT CIRCUIT

The optimum performance of a varactor diode depends to a large extent upon the physics of the device. In Fig. 1, the junction is constructed by solid-state impurity diffusion into a substrate. The mesa varactor structure shown was chosen because of its inherently superior mechanical stability as compared with point-contact structures. It is possible that further improvement might be obtained with epitaxially grown layers, but data on these structures are not yet available.

The equivalent circuit of the varactor diode shown in Fig. 2 includes the electrical properties of both the junction and the package. The capacitance and inductance of the package are assumed to be constant over a wide temperature range. The dissipative resistance of the package is a function of frequency; although it is negligible at low frequencies, it becomes appreciable in the microwave frequency range.

The diode series resistance $R_d(f)$, also a function of frequency, is the sum of the resistances of the semiconductor material on both sides of the junction and the contact resistances. Although $R_d(f)$ decreases slightly at elevated temperatures, it is assumed to be constant over the temperature range considered to simplify the analysis.

Because the package capacitance C_p, and inductance L_p, are lossless elements, they are not considered in the evaluation of the varactor diodes. The package dissipative resistance $R_p(f)$ is included because it can seriously limit performance if it is excessively high.

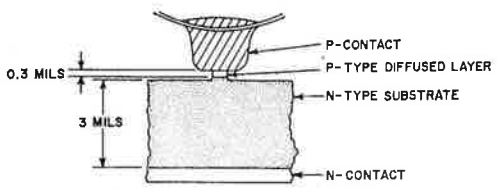

Fig. 1—Varactor diode.

The total series dissipative resistance $R_s(f)$, therefore, is the sum of the package and diode resistances:

$$R_s(f) = R_p(f) + R_d(f) \qquad 1$$

This quantity will be used in the evaluation of the quality factor Q.

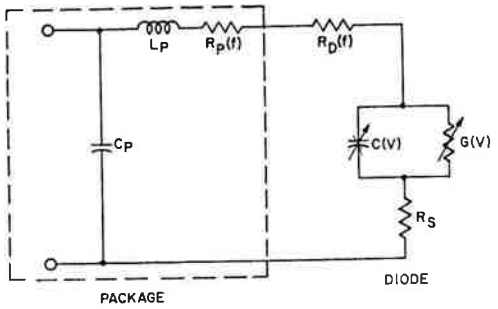

Fig. 2—Equivalent circuit.

The equivalent circuit of the diode itself is represented by the series resistance $R_d(f)$ in series with the parallel arrangement of the junction capacitance $C(V)$ and the junction shunting conductance $G(V)$. (The two latter quantities are functions of voltage.) A high-performance diode for the microwave frequency range must have a junction capacitance $C(V)$ of the order of 1 pf or less. Therefore, the junction shunting conductance $G(V)$ is negligible in the reverse-bias region, and the reverse current is small over the dynamic range employed as compared to the component of current through the capacitance in the microwave frequency region. The equivalent circuit of the diode alone can thus be considered as a series resistive-capacitive circuit.

VARACTOR-DIODE FIGURES OF MERIT

From the various groups working with parametric amplifiers within RCA, several figures of merit for predicting circuit performance have been evolved. The quality factor Q mentioned above is defined as:

$$Q(V,f) = \frac{1}{2\pi f R_s(f) C(V)} \qquad 2$$

Q is defined for a particular frequency value and bias point. It is a function of frequency both explicitly and through the total series resistance $R_s(f)$; it is a function of voltage through the junction capacitance $C(V)$ at the bias point.

An alternate figure of merit which may be derived from Eq. 2 is the frequency for which Q is unity, or the cutoff frequency f_{co} at the bias point:

$$f_{co}(V,f) = \frac{1}{2\pi R_s(f) C(V)} \qquad 3$$

This quantity is preferred by some investigators because it is not as strong a function of frequency as is Q.

There is no generally accepted voltage at which Q and f_{co} are evaluated. Uhlir[1] has suggested the point at which $C(V)$ is a minimum, i.e., the reverse breakdown voltage. In the evaluations reported in this paper, the more conservative —1 and —6 volts are used.

A third figure of merit is the exponent n used in the following junction capacitance-voltage expression[2]:

$$C(V) = \frac{K}{(\Phi_0 - V)^n} \qquad 4$$

Where: K is independent of voltage and Φ_0 is the junction built-in voltage. The value of Φ_0 is approximately 1 volt for the gallium arsenide diodes discussed in this paper. The constant K depends on the dielectric constant of the semiconductor material used, the impurity concentration, and the type of junction (abrupt or graded). The value of n is approximately $\frac{1}{2}$ for abrupt junctions and $\frac{1}{3}$ for graded junctions.

A fourth figure of merit is the capacitance ratio $\Delta C/C$, defined as:

$$\frac{\Delta C}{C} = \frac{C_{(-1)} - C_{(-6)}}{C_{(-1)}} \qquad 5$$

This quantity is sometimes preferred by circuit-design engineers because it is easily measured and provides a convenient indication of junction

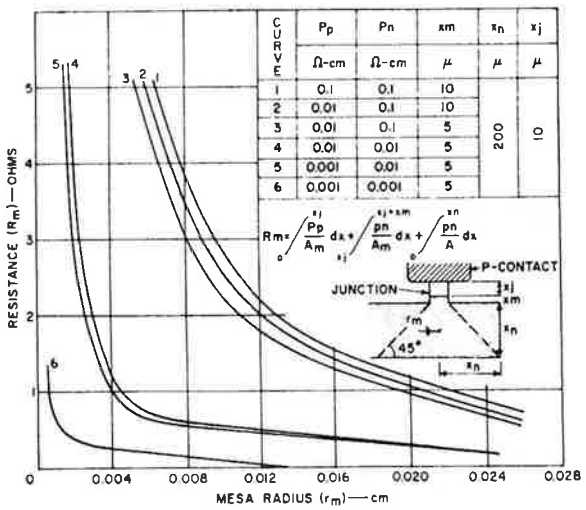

Fig. 3—R_m vs. mesa radius.

DEFINITION OF TERMS

A	Junction area, cm²
C	Junction capacitance, farads
C_p	Package capacitance, farads
f	Operating frequency, cps
f_{co}	Frequency cutoff, measured at microwave frequencies including package losses, cps
G_t	Total conductance, mhos
G	Junction shunting conductance, mhos
K	Constant in capacitance-voltage relation
L_p	Package inductance, henries
n	Exponent in capacitance-voltage relation
Q	Quality factor of diode
Q_s	Quality factor of diode at signal frequency
R_c	Contact resistance, ohms
R_d	Diode series resistance, ohms, measured ta microwave frequencies.
R_m	Resistance of semiconductor material, ohms
R_p	Package dissipative resistance, ohms
R_s	Total series dissipative resistance, ohms, measured at microwave frequencies.
V_p	Pump voltage, volts
V_B	Breakdown voltage, volts
ω_s	Signal frequency, rad/sec
r_m	Radius of mesa, cm
x_j	Junction depth, cm
x_m	N-doped region of mesa
x_n	Base region of diode
ρ_n	Resistivity of n-region, ohm-cm
ρ_p	Resistivity of p-region, ohm-cm
ϕ_o	Built-in potential of diode, volts

characteristics in terms of a circuit parameter. Eq. 4 shows that the ratio $\Delta C/C$ is a function of both n and Φ_o at zero bias; there is a marked dependence on n, but relatively little on Φ_o. Table I lists values of $\Delta C/C$.

DIODE DESIGN CONSIDERATIONS

To achieve gain in a negative-resistance amplifier, it is necessary that the total conductance be negative. The total conductance G_t for a parametric amplifier is:

$$G_t = -\frac{1}{2}\omega_s V_p \frac{dC}{dV} + \frac{\omega_s C}{Q_s} \qquad 6$$

Because the value of C is usually determined by the impedance level required in the circuit, it is desirable to make Q_s, V_p, and dC/dV relatively large.

To fabricate diodes having a high value of Q_s, it is necessary to make the capacitance and the diode series resistance small. The contribution of the semiconductor material to the diode series resistance R_d can be determined from a simple model. R_d can be separated into two parts, as follows:

$$R_d = R_c + R_m \qquad 7$$

Where: R_c is the contribution of the contact resistances and R_m is the contribution of the semiconductor material. The following expression for R_m can be obtained from Fig. 3:

$$R_m = \frac{\rho_p}{\pi r_m^2} x_j + \frac{\rho_n}{\pi r_m^2} x_n + \int_o^{x_n} \frac{\rho_n}{A}\, dx \qquad 8$$

The first term in this expression represents the p-region part of the mesa, the second the n-type part of the mesa, and the last the spreading resistance. Because of the impurity diffusion conditions the resistivity p_p is usually very small; the resistivity p_n is dictated in part by the breakdown voltage required.

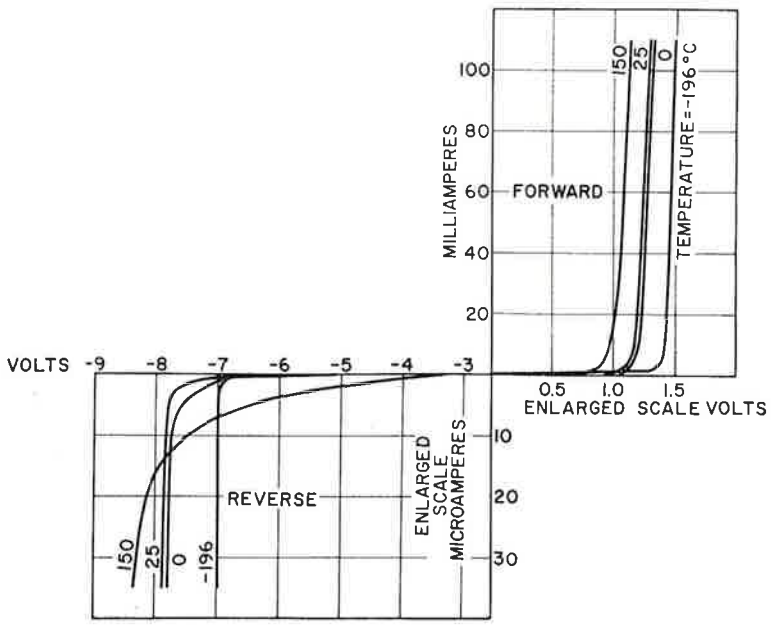

Fig. 4—V-I characteristics.

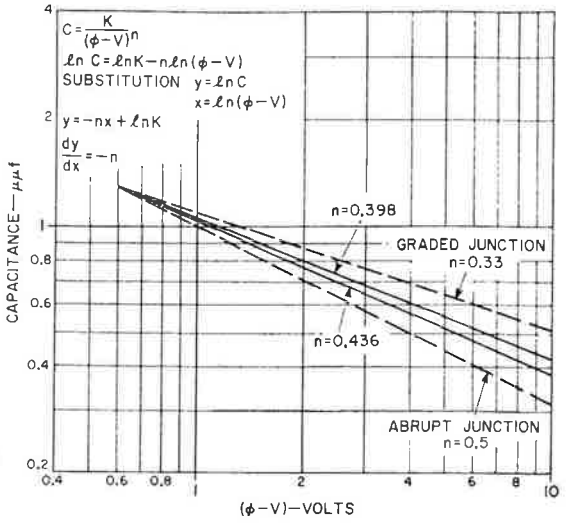

Fig. 5—Junction capacitance vs. voltage. Solid: usual n values for GaAs varactor diodes. Dashed: extreme cases for abrupt and graded junctions.

Fig. 3 shows several curves of R_m as a function of mesa radius r_m for several sets of parameters. The mesa area is the dominant factor in the expression for R_m when the resistivities on both sides of the junction are small; therefore, R_m rises sharply for small mesa radius. When the resistivity on either side of the junction is high, however, R_m is insensitive to mesa radius.

Values of contact resistance are usually quite small in germanium and silicon devices, but not in GaAs units. In the varactor diode shown in Fig. 1, the contribution R_m is usually less than R_c. Experimental data show that R_c is usually of the order of 0.5 ohm when measured under dc conditions. Contact resistance is not negligible, therefore, although it is not the dominant factor in the diode series resistance.

For junction penetrations of 0.2 to 0.3 mil, it has been experimentally determined that the R_dC product is minimized for values of capacitance less than 1 pf. In most applications above 1 Gc, the impedance level in microwave systems also requires capacitance values less than 1 pf. The GaAs varactor diodes described in this paper have capacitance values ranging from 0.1 to 1.0 pf. The highest-Q diodes employing the most up-to-date geometry usually exhibit values of 0.3 pf or less.

The magnitude of the negative conductance G_t is also proportional to the capacitance-voltage sensitivity dC/dV. Eq. 6 can be rewritten:

$$G_t = -\omega_s C\left[\frac{1}{2}\,\frac{V_p}{C}\,\frac{dC}{dV}-\frac{1}{Q_s}\right] \qquad 9$$

In this equation, the important parameter showing the fractional change of capacitance with respect to voltage is obtained from Eq. 4:

$$\frac{1}{C}\,\frac{dC}{dV}=\frac{n}{\Phi_o-V} \qquad 10$$

Thus the capacitance-voltage sensitivity is proportional to the exponent n. As mentioned previously, the value of n is $\frac{1}{2}$ for an abrupt junction and $\frac{1}{3}$ for a graded junction. For the junction used in the GaAs varactor diodes, in which the impurity concentration is neither abrupt nor graded, n lies between $\frac{1}{2}$ and $\frac{1}{3}$.

TABLE I—Calculated Values Fractional Change of Junction Capacitance of GaAs Diodes for Abrupt and Graded Junctions.

Δ·C/C	Φ_o=0.9 v	Φ_o=1.0 v	Φ_o=1.1 v
Abrupt	0.475	0.466	0.456
Graded	0.350	0.342	0.334

A compromise must be made in varactor diodes between the series resistance R_d and the breakdown voltage V_b (voltage at which the leakage current is 10 μa). Although lower concentrations and/or diffusion times result in greater breakdown voltages, they also increase the series resistance. The minimum breakdown voltage required to accommodate 200 mw of pump power at 35 Gc for an X-band parametric amplifier is 6 volts. Breakdown voltages as high as 40 volts have been achieved with the design described, with cutoff frequencies of about 200 Gc at —1 volt.

EXPERIMENTAL RESULTS

Fig. 4 shows the voltage-current characteristics of typical GaAs arsenide varactor diodes at four temperatures ranging from 150 to —196°C. The variation of breakdown voltage at either temperature extreme is less than 15 per cent of the value at 25°C. Reverse leakage current is less than 10^{-7} ampere for reverse voltages below the breakdown value for temperatures of 100°C or less.

TABLE II—Measurements of GaAs Varactor Diodes

Diode	V_B v @ 10μa	C pf	$\Delta C/C$ fig. of merit	R_S ohms	f_{co} Gc	f^*_{co} G_c
† At 2 Gc, −6v:						
1	12.1	0.260	0.48	1.48	>250	414
2	10.8	0.295	0.42	1.21	>250	445
3	10.4	0.315	0.39	0.93	>250	546
4	9.9	0.249	0.41	1.75	>250	366
At 10 Gc, −6v:						
5	10.0	0.30	0.39	3.12	170	—
6	10.0	0.24	0.37	3.35	198	—
7	11.6	0.35	0.42	2.22	170	—
8	13.4	0.28	0.5	0.64	893	—
9	11.8	0.24	0.36	1.92	346	—

* Actual measured
† Capacitance values @ 1 Mc

TABLE III—Performance of GaAs Varactor Diodes

Signal Frequency, Gc	9.375	8.7
Pump Frequency, Gc	35.8	35.0
Gain, db	15	10
Bandwidth, Mc	16.0	200
Noise Figure, db	2.8*	2.9
Pump Power, mw	125	180

* Includes 2-db circulator loss.

The breakdown characteristic is sharp except at temperatures approaching 150°C. The knee of the forward characteristic becomes sharper with decreasing temperature; this effect is caused by an increase in the junction built-in voltage as the temperature is reduced.

Fig. 5 shows the junction capacitance vs. voltage for typical diodes. The magnitude of the slope of each curve is proportional to the exponent *n;* larger slopes result in greater capacitance-voltage sensitivity. It can be seen that the slope of the solid curves is superior to that of graded junctions, and approaches that of abrupt junctions.

The slope of the capacitance curve is also dependent to some extent on the value of Φ_o, although little effect was noted in Table I in the voltage range from 0.9 to 1.1 volt. Data are usually plotted for several values of Φ_o, and the value which provides the best straight line is taken as the junction built-in potential. This value is usually about 1.0 volt for GaAs devices. The experimental values measured for n indicate that the impurity profile lies between the abrupt and erfc profiles.

In the early stages of the development programme, cutoff frequency was measured at 2 Gc using a slotted-line technique. With this equipment, however, values above 250 Gc are not accurate. Table II shows data for several diodes measured at 2 Gc and —6 volts (diodes 1-4). Actual measured cutoff frequencies are shown (f_{co}*). For diodes 1-4, junction capacitance values (measured at 1 Mc) were less than 0.32 pf, and values of total series resistance were less than 1.75 ohms; also, because the dissipative resistance of the package is less than several tenths of an ohm, the package microwave losses are not large.

Table II also shows measurements made on several GaAs varactor diodes (diodes 5-9) at 10 Gc and —6 volts. The dissipative resistances shown in the table represent total diode and package resistance. No satisfactory method is available for determining separate resistance values at 10 Gc.

Table III shows typical results obtained when these GaAs varactor diodes were used in X-band nondegenerate negative-resistance parametric amplifiers. The cutoff frequency of the diodes was high enough to permit the use of a pump frequency of 35 Gc. In addition, the capacitance-voltage sensitivity of the diodes permitted the use of a relatively low pump power level to achieve adequate gain. The capacitance-voltage sensitivity is also reflected to some extent in the low noise figures. If the sensitivity were too low to achieve gain, the pump power would have to be increased, thus increasing noise.

As shown in Table III, a larger bandwidth can be used if less gain can be tolerated. This exchange of characteristics is possible because the parasitic capacitance and inductance values of the package are quite low.

CONCLUSIONS

It has been shown that very-high-cutoff-frequency diodes may be fabricated from GaAs. Typical values exceed 250 Gc and are significantly higher than values reported in the literature. The *V-I* characteristic indicates little change in the temperature range from —196 to approximately 100°C. Cutoff frequency and the capacitance-voltage sensitivity are adequate figures of merit to guide design considerations for use of varactors in parametric amplifiers. The circuit-performance gain, bandwidth, and noise figure are outstanding.

ACKNOWLEDGEMENT

The authors are pleased to acknowledge the permission of A. Solomon to publish the data in the first column and of R. J. Kampf and V. D. Holaday to publish the data in the second column in Table III, and of H. C. Lee to publish the data in Table II for diodes 5-9.

A portion of the work described was performed under the sponsorship of the Electronic Technology Laboratory, Aeronautical Systems Div., Systems Command, USAF.

BIBLIOGRAPHY

1. A. Uhlir, Jr., "The Potential of Semiconductor Diodes in High-Frequency Communications," *Proc. IRE,* Vol. 46, p. 1099, June, 1958.
2. W. Shockley, "The Theory of p-n Junctions in Semiconductors and p-n Junction Transistors," *Bell Sys. Tech. Jour.,* Vol. 28, p. 435, July, 1949.
3. J. Hilibrand and W. R. Beam, "Semiconductor Diodes in Parametric Subharmonic Oscillators," *RCA Review,* Vol. XX, p. 229, June, 1959.

(With acknowledgements to RCA)

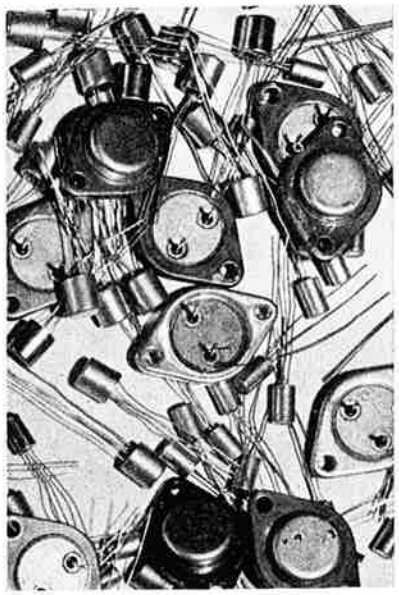

THE TRANSISTOR "FAMILY" CONCEPT

In May of 1961, we published in these pages data on the AWV transistor families as they then were. Since then there have been several changes. New types have been introduced, and in fact complete new families. It seems appropriate therefore, in view of the interest that resulted from the first publication, that a revised edition of the story should be prepared and published. This, then, is the 1963 AWV Transistor Family.

It is general knowledge these days that transistors are manufactured in "families", and that tests applied after manufacture select the finished units into groups bearing the various commercial type numbers within the particular family. In this way the manufacture of transistors differs from the manufacture of thermionic valves, where a discrete type is made.

There may be as many as ten or more transistors identified by different commercial type numbers, but belonging to a family group, and all stemming from the same manufacturing run. This fact arises from the complex nature of the doping and other processes that are used to make a transistor, and from the minute variations in material properties needed to produce transistors of varying characteristics.

These considerations mean that whilst it would be possible to set out to make one discrete type of transistor, it is neither a practical nor an economic procedure. The "family" concept of transistor production, which is common to all transistor manufacturers, by easing manufacturing problems and ensuring maximum utilization of expensive raw materials, brings the user a high-grade product at a moderate price.

Furthermore, the stringent testing applied in the selection of the finished units into categories representing the various commercial type numbers, brings the user another advantage. The tests result in a finished and branded product which offers the user closer limits, with all their attendant advantages, than would otherwise be feasible.

In order for the user to gain the maximum benefit from the advantages of "family" manufacturing techniques, it is of course necessary for him to understand the properties which decide the final type numbering of the members of a group. In

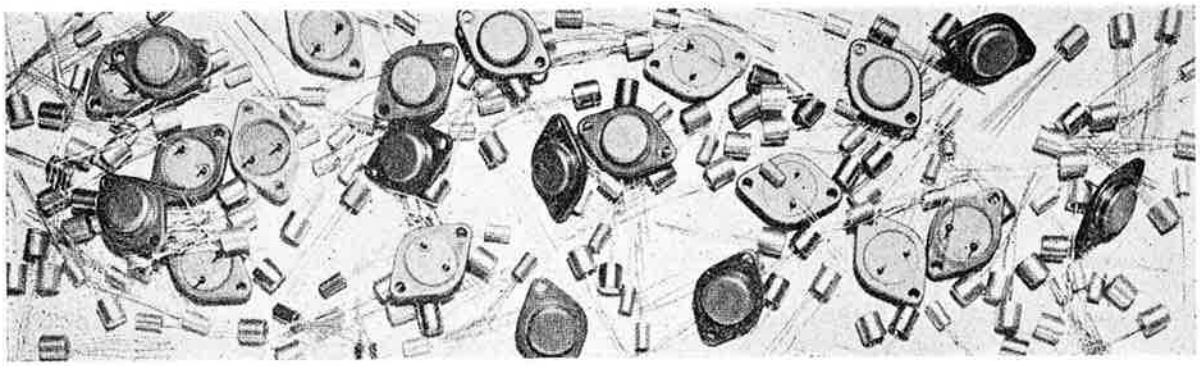

this way the most suitable choice can be made, having regard to the job the transistor has to do, and to factors such as price and availability.

The "family trees" presented here show how some of the more popular AWV transistors and silicon diodes are grouped together, and how the characteristics are selected within each group. If, for example, a transistor is required for an audio application, the AUDIO FAMILY chart immediately shows, not only the possible types available, but also guides the selection towards the most suitable type. Naturally, the final selection would be made after a more detailed examination of the transistor's characteristics.

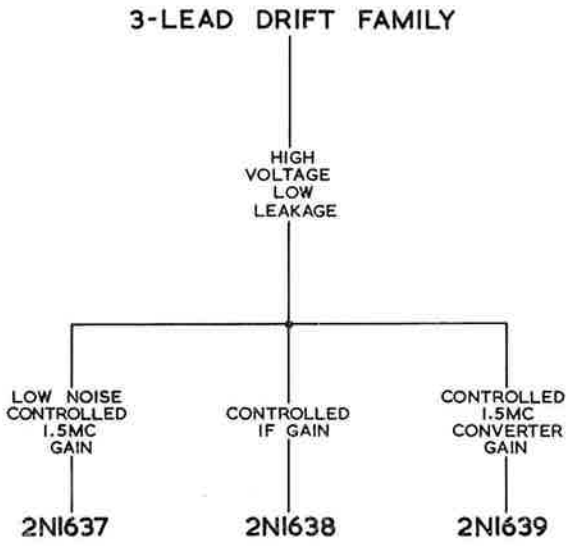

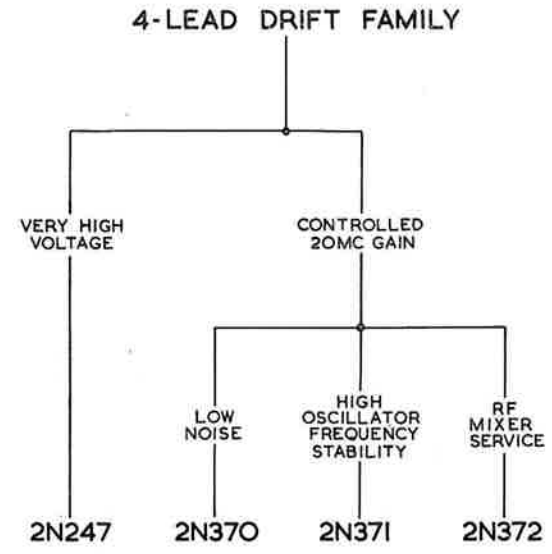

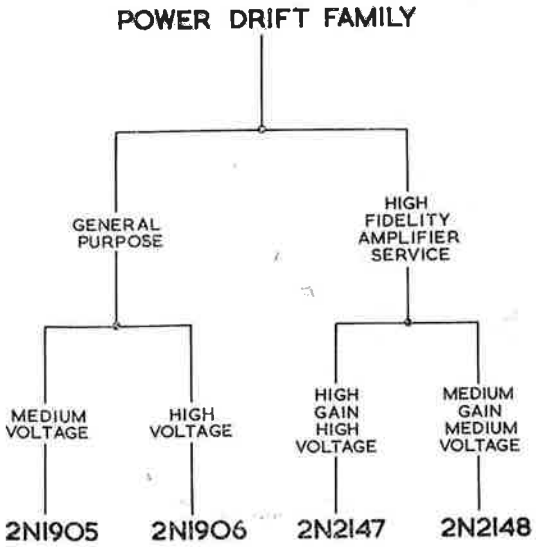

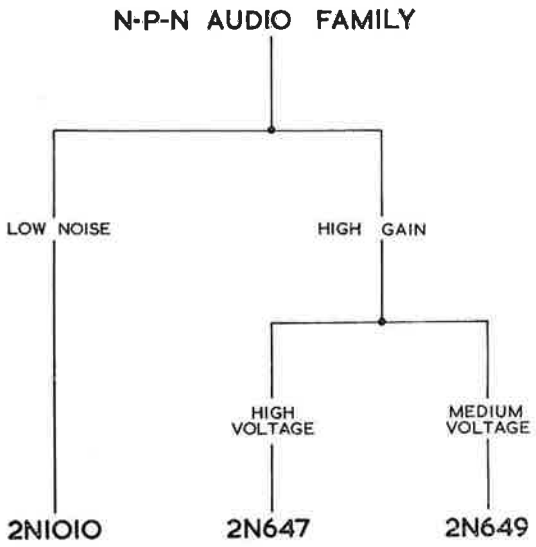

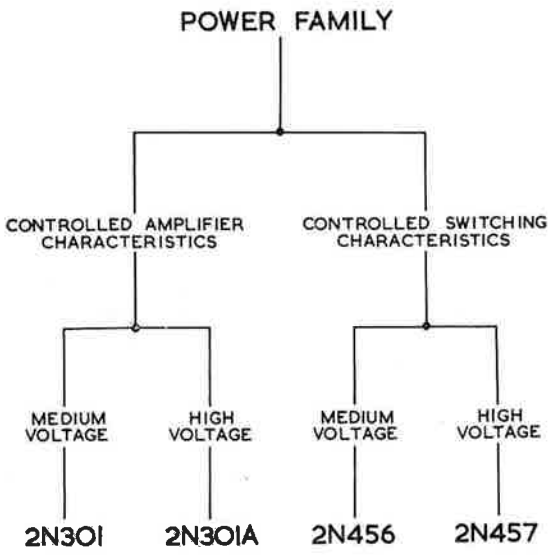

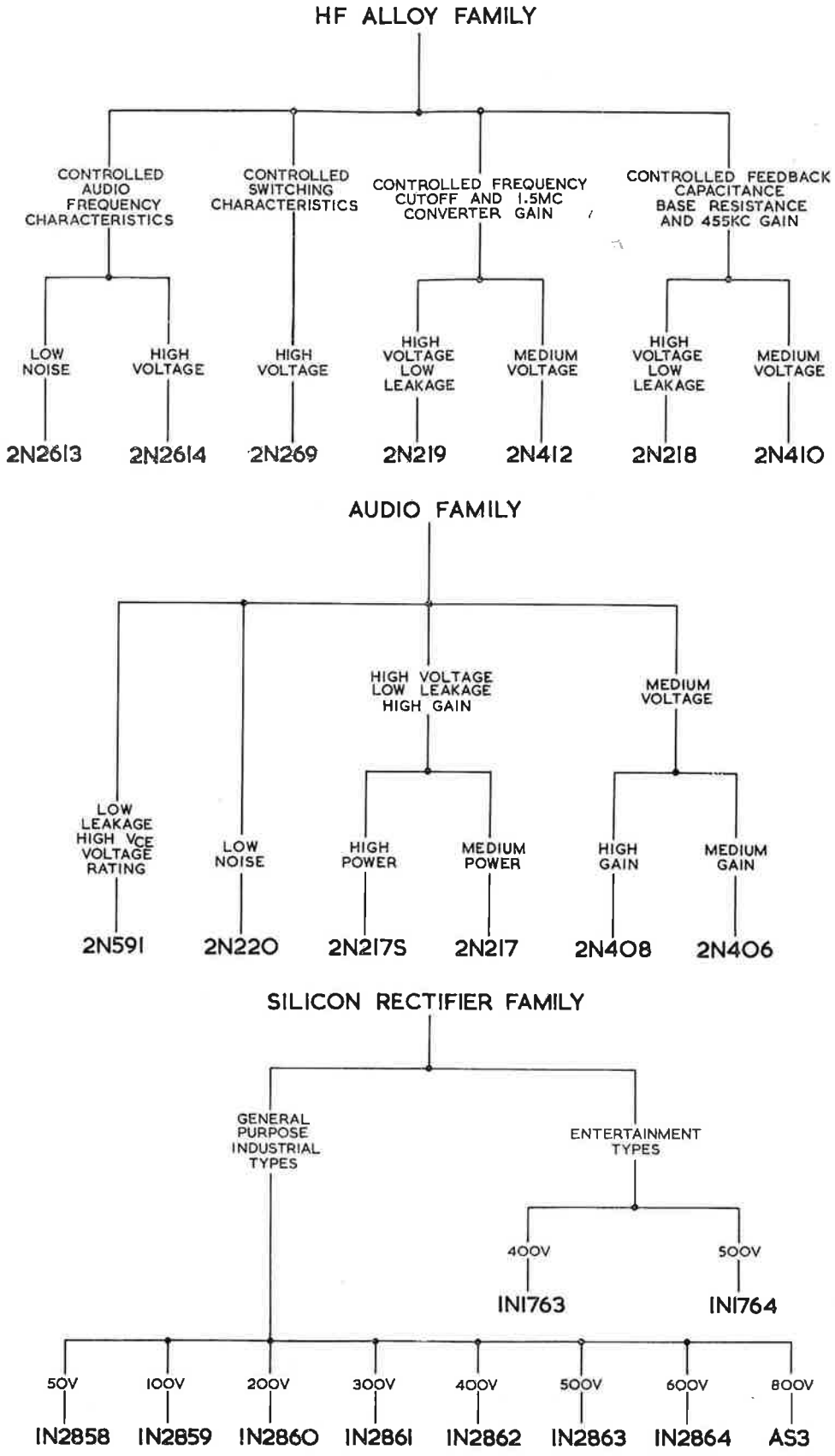
HF ALLOY FAMILY
CONTROLLED AUDIO FREQUENCY CHARACTERISTICS
CONTROLLED SWITCHING CHARACTERISTICS
CONTROLLED FREQUENCY CUTOFF AND 1.5MC CONVERTER GAIN
CONTROLLED FEEDBACK CAPACITANCE BASE RESISTANCE AND 455KC GAIN
LOW NOISE
HIGH VOLTAGE
HIGH VOLTAGE
HIGH VOLTAGE LOW LEAKAGE
MEDIUM VOLTAGE
HIGH VOLTAGE LOW LEAKAGE
MEDIUM VOLTAGE
2N2613
2N2614
2N269
2N219
2N412
2N218
2N410
AUDIO FAMILY
HIGH VOLTAGE LOW LEAKAGE HIGH GAIN
MEDIUM VOLTAGE
LOW LEAKAGE HIGH VCE VOLTAGE RATING
LOW NOISE
HIGH POWER
MEDIUM POWER
HIGH GAIN
MEDIUM GAIN
2N591
2N220
2N2175
2N217
2N408
2N406
SILICON RECTIFIER FAMILY
GENERAL PURPOSE INDUSTRIAL TYPES
ENTERTAINMENT TYPES
400V
500V
IN1763
IN1764
50V
100V
200V
300V
400V
500V
600V
800V
IN2858
IN2859
IN2860
IN2861
IN2862
IN2863
IN2864
AS3

MODULATION WITH TUNNEL DIODES

B. RABINOVICI, Ldr., S. KALLUS, J. KLAPPER

Systems Laboratory Surface Communications Division, DEP, New York, N.Y.

Inherent tunnel-diode characteristics are advantageously used herein to design a single-tunnel-diode suppressed-carrier modulator, and a two-tunnel-diode balanced modulator that acts as a ring modulator with proper biasing. Both require low carrier and modulating power, making them suitable for low signal levels.

The nonlinear current-voltage characteristic and negative dynamic-conductance region of tunnel diodes offer the possibility of modulation with gain, normally achieved by use of transistors and electron valves. Further, the unique characteristic of the tunnel diode, nearly parabolic at the current peak, permits the design of very simple suppressed-carrier modulators.

Previously, carrier suppression was obtained by the use of carefully balanced circuits with two conventional diodes; a single-tunnel-diode modulator, properly biased, gives an equivalent carrier suppression. Similarly, ring-type modulators with conventional diodes use a double-balanced circuit with four diodes; two tunnel diodes, properly biased and in a balanced arrangement can give equal performance.

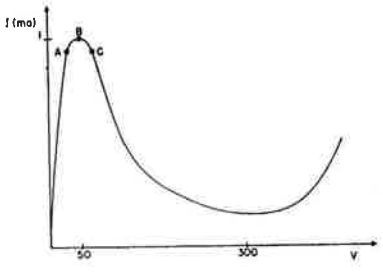

Fig. 1—Typical germanium tunnel-diode characteristic.

A linear equivalent circuit for the nonlinear modulation process can be used to calculate the performance of the modulators.

LINEAR EQUIVALENT CIRCUIT

Fig. 1 shows a typical tunnel diode *I-V* characteristic.[1] The tunnel-diode modulators described herein operate in the region *A-B-C* of the characteristic. This region may be approximated by the first two terms of a power series:

$$i = G_o v - g v^2 \qquad 1$$

Where: i and v = current and voltage variations, respectively, about the bias point; and G_o = dynamic conductance at the bias point.

Fig. 2 is a simplified schematic diagram of a tunnel-diode modulator. If sinusoidal voltages

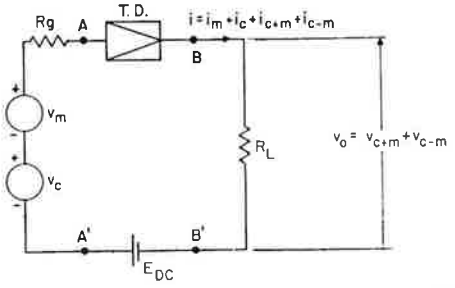

Fig. 2—Tunnel-diode modulator simplified schematic.

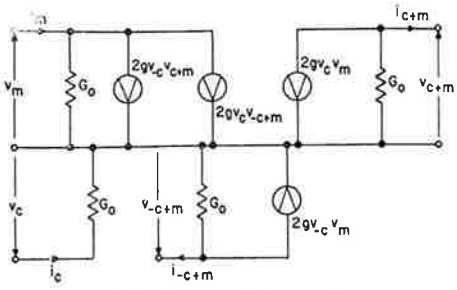

Fig. 3—Tunnel-diode modulator, linear equivalent circuit.

and small-signal conditions are assumed, the current-voltage relationships of the tunnel diode are given in matrix form as:

$$\begin{bmatrix} i_m \\ -i_{c+m} \\ -i_{-(c-m)} \\ i_c \end{bmatrix} = \begin{bmatrix} G_o & 2gV_{-c} & 2gV_c & O \\ 2gV_c & G_o & O & O \\ 2gV_{-c} & O & G_o & O \\ O & O & O & G_o \end{bmatrix} \times \begin{bmatrix} V_m \\ V_{c+m} \\ V_{-(c-m)} \\ V_c \end{bmatrix} \quad 2$$

Matrix 2 represents the current-voltage relationship of the tunnel-diode modulator, containing one equation for each frequency component of interest. The matrix shows a linear relationship between the currents and voltages of the tunnel-diode at the frequencies ω_m, ω_c, and $\omega_c \pm_m$. Therefore, a linear equivalent circuit can be constructed which represents the tunnel-diode modulator. This linear equivalent circuit (Fig. 3) makes it possible to apply the well-developed linear-circuit techniques to a modulation process that is inherently nonlinear. Note that in agreement with the physical picture, the input and output voltages are mutually coupled by the carrier voltage.

Through linear-circuit analysis techniques, the performance criteria of the tunnel-diode modulator are as follows:

Input Admittance:

$$Y_{in} = G_o - \frac{2(\Delta G)^2}{G_o + G_L} \quad 3$$

Output Admittance:

$$Y_{out} = G_o - \frac{2(\Delta G)^2}{G_o + G_g} \quad 4$$

Voltage Gain:

$$A_v = \frac{V_{c\pm m}}{V_m} = -\frac{\Delta G}{G_o + G_L} \quad 5$$

Power Gain:

$$A_p = \frac{8G_gG_L(\Delta G)^2}{\left[(G_o + G_g)(G_o + G_L) - (\Delta G)^2\right]^2} \quad 6$$

Where: ΔG = change in the tunnel-diode conductance introduced by the carrier swing, and G_g, G_L = generator and load conductances, respectively.

SUPPRESSED-CARRIER MODULATION

The single-tunnel-diode circuit can give suppressed-carrier modulation. In Fig. 1, the region *A-B-C* is very nearly parabolic. The even symmetry can be further enhanced by choosing the proper value of the load resistor. For the 1-ma tunnel diode used, a 27-ohm load resistor was found to yield the optimum curve.

Suppressed-carrier modulation is achieved by biasing the tunnel diode at the peak of the *I-V* curve. Note that at the peak there is 1) *zero conductance* (i.e. zero slope), and 2) *even symmetry about the peak.* When the tunnel diode is biased at the peak of its *I-V* characteristic, its dynamic conductance, G_o, is zero. It can be seen from matrix 2 that when $G_o = 0$, no current flows at the carrier frequency. The even symmetry is important in order to avoid a carrier-frequency current component due to odd higher-order curvatures.

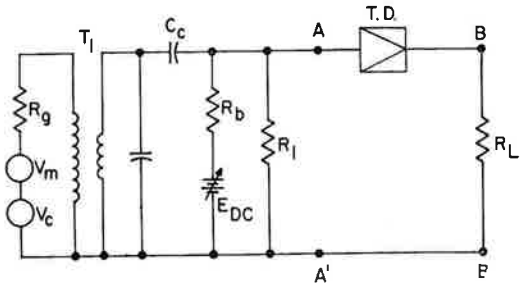

Fig. 4—Tunnel-diode suppressed-carrier modulator, simplified schematic.

Fig. 4 is a schematic of a single-tunnel-diode suppressed-carrier modulator which was built. The measured sideband-to-carrier ratio at the output was 40 db with a gain of about 2 db. The carrier level at the output is about 70 db below that at the input.

BALANCED MODULATION

Fig. 5 is a simplified schematic diagram of a tunnel-diode balanced modulator. Proceeding in the same manner as for the single-tunnel-diode modulator, but taking the output current as the difference between the currents of the individual tunnel diodes, the current-voltage relationships are in the form:

$$\begin{bmatrix} i_m \\ -i_{c+m} \\ -i_{-(c-m)} \end{bmatrix} = \begin{bmatrix} 2G_o & 4gV_{-c} & 4gV_c \\ 4gV_c & 2G_o & O \\ 4gV_{-c} & O & 2G_o \end{bmatrix} \times \begin{bmatrix} V_m \\ V_{c+m} \\ V_{-(c-m)} \end{bmatrix} \quad 7$$

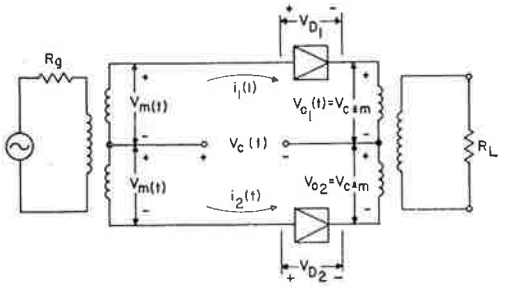

Fig. 5—Tunnel-diode balanced modulator, simplified schematic.

This matrix is identical to matrix 2 except that G_o is replaced by $2G_o$, and g by $2g$. Note that the carrier component of current is zero even though the tunnel diodes are not necessarily biased at the peak. This is because the two tunnel diodes were assumed to be identical and biased at the same point, the usual manner of achieving suppressed-carrier modulation with other devices.

Fig. 6 is the linear equivalent circuit representing matrix 7. The performance equations for this modulator are:

Input Admittance:

$$Y_{in} = 2G_o - \frac{2\,(2\Delta G)^2}{G_L + 2G_o} \qquad 8$$

Output Admittance:

$$Y_{out} = 2G_o - \frac{2\,(2\Delta G)^2}{G_g + 2G_o} \qquad 9$$

Voltage Gain:

$$A_v = -\frac{2\Delta G}{G_L + 2G_o} \qquad 10$$

Power Gain:

$$A_p = \frac{8G_gG_L\,(2\Delta G)^2}{\left[(G_g + 2G_o)(G_L + 2G_o) - (2\Delta G)^2\right]^2} \qquad 11$$

RING MODULATION

The tunnel-diode balanced modulator described above acts as a ring modulator, if the tunnel diodes are biased at the peak of the *I-V* characteristic.

The current is an even function of voltage when the tunnel diode is biased at the peak of the *I-V* curve and the load resistor is properly chosen. Therefore, the *I-V* curve can be expressed as a power series:

$$i = \sum_{n=0}^{\infty} a_n V^n \qquad 12$$

Where a_n is related to the nth derivative (n even) at the operating point and V is the voltage across the tunnel diode. The output current is the difference between the currents of each tunnel diode and may be expressed in the form of a series with the nth term given by:

$$i_n = 2a_n \left[nV_c^{n-1}V_m + \frac{n\,(n-1)\,(n-2)}{3!}V_c^{n-3}V_m^3 \cdots \right.$$
$$\left. \cdots + \frac{n!}{(n-r)!\,r!}V_c^{n-r}V_m^r + \cdots \right] \qquad 13$$

Where: r is always an odd integer as a result of the balanced circuit arrangement. Since n is an even integer as described above, $(n\text{-}r)$ is always odd. If this term is expanded (recalling that V_c and V_m are sinusoidal), then the only terms appearing at the output are odd-order sidebands spaced around odd multiples of the carrier frequency. This is tantamount to ring modulation, which is normally accomplished with four nonlinear elements in a bridge-type arrangement.[2]

The physical picture of this ring-modulation process may be conceived in the following manner: When a tunnel diode is biased at the peak of its *I-V* characteristic, it has some properties of a balanced circuit, as seen in reference to its carrier-suppression capabilities. Two such circuits in a balanced arrangement are, therefore, equivalent to a double balanced arrangement—another expression for ring modulation.

In the tunnel-diode ring modulator that was constructed, the sideband-to-carrier ratio measured was 50 db. The second-order sidebands were 62 db below the primary sideband level, and the second harmonic of the carrier was 40 db lower than for the single-tunnel-diode modulator.

CONCLUSIONS

A single tunnel diode, biased at the peak of its *I-V* characteristic, offers a 40-db sideband-to-carrier ratio—normally achieved by a pair of matched nonlinear active elements.

Ring modulation is accomplished with two tunnel diodes in a balanced circuit, both diodes being biased at the peak of their *I-V* characteristics—normally achieved by four nonlinear elements in a bridge arrangement. If the tunnel diodes are equally biased, but not at the peak, only balanced operation is obtained.

Both modulators require low carrier and modulating power when biased at the peak of their *I-V* characteristics, where $G_o = 0$. This makes them suitable for low-signal-level applications. The power-handling capability of the modulators is rather low for the 1-ma tunnel diode (IN2939) used; however, it could be increased by using

tunnel diodes with higher peak-current characteristics.

BIBLIOGRAPHY

1. L. Esaki, "New Phenomenon in Narrow Ge p-n Junctions," *Phys. Rev.*, vol. 109, p. 603 (L) 1958.
2. R. S. Caruthers, "Copper Oxide Modulators in Carrier Telephone Systems," *Trans. AIEE*, pp. 253-260, June, 1939.

(With acknowledgements to RCA)

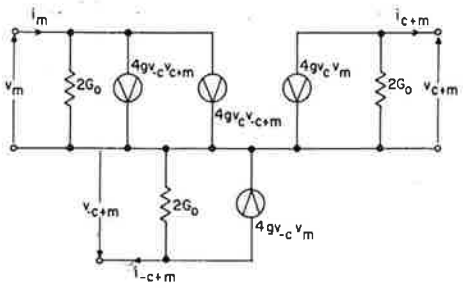

Fig. 6—Tunnel-diode balanced modulator, linear equivalent circuit.

NEW TUNNEL DIODES 1N3847-1N3860 TUNNEL RECTIFIERS 1N3861-1N3862

For Switching, Small-signal and Coupling Application

Types 1N3847 through 1N3860 are germanium epitaxial tunnel diodes designed for a wide range of requirements in high-speed switching and high-frequency small-signal applications. These devices provide typical switching speeds ranging from 75 picoseconds to 1800 picoseconds, tightly controlled peak-point currents (±5%, ±10%), and dissipation capabilities from 10 mw to 100 mw. All types feature low-capacitance, epitaxially grown junctions, and all-ceramic-and-metal package for very low inductance.

Tunnel-diode types 1N3856, 1N3857, 1N3858, 1N3859, and 1N3860 are intended for use in extremely critical switching and small-signal applications requiring tight (±5%) control of peak-point currents, and switching speeds as fast as 75 picoseconds.

Tunnel-diode types 1N3852, 1N3853, 1N3854, and 1N3855 are intended for use in switching and small-signal applications requiring tight (±5%) control of peak-point currents, and switching speeds as fast as 200 picoseconds.

Tunnel-diode types 1N3847, 1N3848, 1N3849, 1N3850 and 1N3851 are intended for use in switching and small-signal applications requiring switching speeds as fast as 125 picoseconds, for which a peak-point-current control of ±10% is permissible.

Tunnel-rectifier types 1N3861, 1N3862, and 1N3863 are intended for use as coupling devices in very-high-speed switching applications in memory systems and other critical equipment. These devices feature the same type of all-ceramic-and-metal package as the tunnel diodes described above.

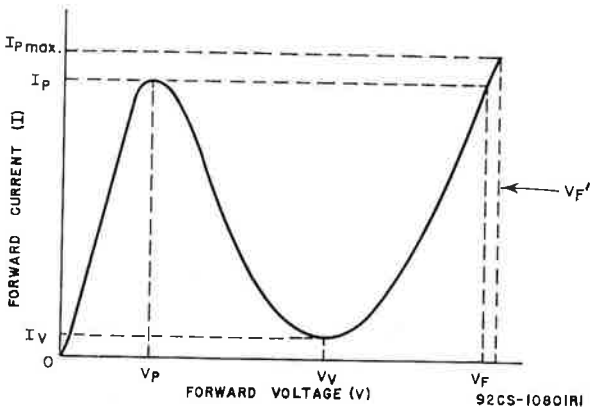

Fig. 1—Static Forward Characteristic of Tunnel Diode.

Maximum Ratings, Absolute-Maximum Values:

	TUNNEL DIODES					TUNNEL RECTIFIERS
	IN3847 IN3852 IN3857	IN3848 IN3853 IN3858	IN3849 IN3854 IN3859	IN3850 IN3855 IN3860	IN3851 IN3856	IN3861 IN3862 IN3863
CONTINUOUS CURRENT (MILLIAMPERES):						
Forward	10	18	35	85	170	10
Reverse	15	25	50	125	250	30
DISSIPATION (MILLIWATTS):						
At T_{FA} = 25° C (Derate linearly to 0 mw at T_{FA} = 100° C)	5	10	20	50	100	10
FREE-AIR TEMPERATURE RANGE (°C):						
Storage and Operating	-35 to +100					
LEAD TEMPERATURE (°C):						
For 3 seconds max. (See Soldering Instructions)	175					

Electrical Characteristics, at Ambient Temperature = 25°C:

TUNNEL DIODES

Type	I_P ma		I_V ma	I_P/I_V	V_P mv		V_V mv	V_F' mv		C^a pf	R_S ohms	t_r psec
	Min.	Max.	Max.	Min.	Min.	Max.	Min.	Min.	Max.	Max.	Max.	Typ.
IN3847	4.5	5.5	0.75	6/1	-	-	-	430	590	25	3	1800
IN3852	4.75	5.25	0.6	8/1	50	90	330	490	560	15	3	1200
IN3857	4.75	5.25	0.6	8/1	50	90	330	490	560	8	3	600
IN3848	9	11	1.5	6/1	-	-	-	440	600	25	2.5	900
IN3853	9.5	10.5	1.2	8/1	55	95	350	510	580	15	2.5	600
IN3858	9.5	10.5	1.2	8/1	55	95	350	510	580	8	2.5	300
IN3849	18	22	3	6/1	-	-	-	460	620	30	2	600
IN3854	19	21	2.4	8/1	65	105	365	530	600	20	2	400
IN3859	19	21	2.4	8/1	65	105	365	530	600	10	2	200
IN3850	45	55	7.5	6/1	-	-	-	530	640	40	1.5	350
IN3855	47.5	52.5	6	8/1	80	130	380	550	620	25	1.5	200
IN3860	47.5	52.5	6	8/1	80	130	380	550	620	12	1.5	150
IN3851	90	110	15	6/1	-	-	-	540	650	40	1	125
IN3856	95	105	12	8/1	90	140	390	560	630	25	1	75

[a] Includes case capacitance of 0.8 pf.

TUNNEL RECTIFIERS

Type	I_P ma		C^b pf	V_R mv at I_R = 10 ma	V_R mv at I_R = 30 ma	V_F mv at I_F = 1 ma
	Min.	Max.	Max.	Max.	Max.	Min.
IN3861	0.1	1	6	170	-	400
IN3862	0.1	1	4	150	300	420
IN3863	0.1	0.5	4	150	300	435

[b] Includes case capacitance of 0.4 pf.

DEFINITIONS OF SYMBOLS

The *static characteristic* symbols below for tunnel diodes and tunnel rectifiers are defined with respect to the characteristic curves shown in Fig. 1 and Fig. 2, respectively.

I_F = Static forward current
I_R = Static reverse current
I_p = Peak-point forward current (the value of static forward current I_F flowing at the lowest positive voltage V at which $dI_F/dV = 0$).
I_V = Valley-point current (the value of static forward current I_F flowing at the second lowest positive voltage V at which $dI_F/dV = 0$).
I_p/I_V = Peak-to-valley current ratio
V_p = Peak-point voltage (the lowest value of positive voltage V at which $dI_F/dV = 0$).
V_V = Valley-point voltage (the second lowest value of positive voltage V at which $dI_F/dV = 0$).
V_F = The positive voltage greater than V_V at which the static forward current I_F is equal to the peak-point forward current I_p.
$V_F{}^1$ = The positive voltage greater than V_V at which the static forward current I_F is equal to the maximum specified value of I_p.
V_R = Reverse voltage

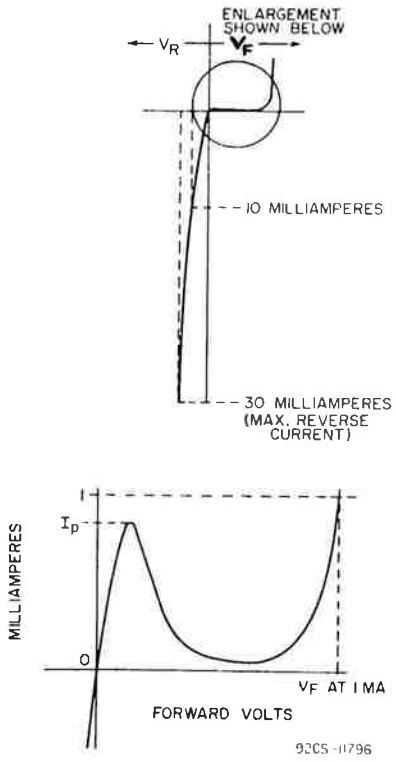

Fig. 2—Static Characteristic of Tunnel Rectifier.

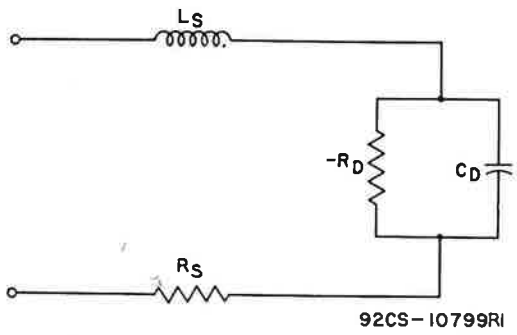

Fig. 3—Equivalent Circuit of a Tunnel Diode in the Negative-Resistance Region.

The *dynamic characteristic* symbols below for tunnel diodes are defined with respect to the equivalent circuit shown in Fig. 3. Because C_D and $-R_D$ are functions of the operating voltage, a statement of the operating voltage is necessary to define the equivalent circuit.

R_S = Total series resistance
L_S = Total series inductance
C = Terminal valley-point capacitance
C_D = Barrier capacitance of the intrinsic diode
$-R_D$ = Negative resistance of the intrinsic diode
t_r = Calculated rise time (approximate) for a germanium tunnel diode when switching from V_p to V_F at a constant value of I_p. Calculated from the relationship

$$t_r \simeq \frac{C\,(V_F - V_p)}{(I_p - I_V)} \simeq \frac{C}{2\,I_p}$$

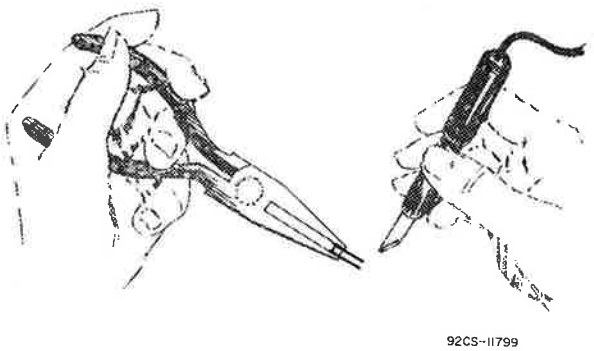

Fig. 4—Suggested method for holding tunnel diode or tunnel rectifier with straight tabs during soldering.

SOLDERING INSTRUCTIONS

A low-temperature solder (such as Alpha #111 alloy, rosin-filled, or equivalent) should be used. The soldering iron tip temperature should not exceed 175°C and soldering time should not exceed 3 seconds. A pre-tinned circuit board should be used to minimize soldering time.

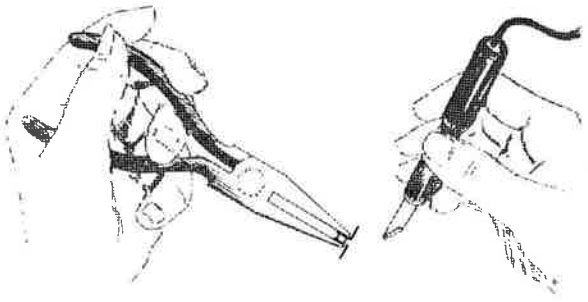

92CS-11798

To protect the junction against overheating, the tunnel diode or tunnel rectifier should be held with long-nose pliers, as shown in Figs. 4 and 5.

Fig. 5—Suggested method for holding tunnel diode or tunnel rectifier with bent tabs during soldering.

DIMENSIONAL OUTLINE
For TUNNEL DIODE Types IN3847 To IN3860

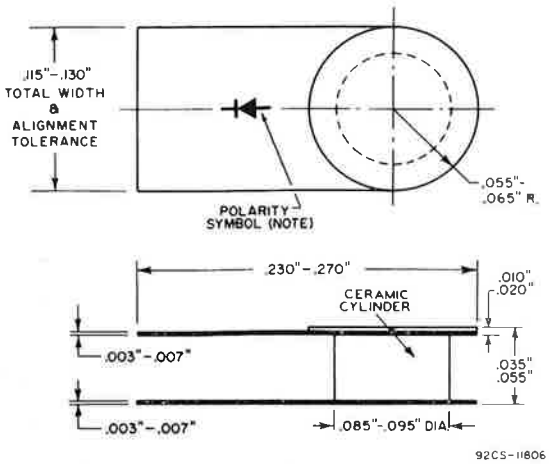

92CS-11806

NOTE: ARROW INDICATES DIRECTION OF FORWARD CURRENT FLOW AS INDICATED BY DC AMMETER.

DIMENSIONAL OUTLINE
For TUNNEL RECTIFIER Types IN3861 To IN3863

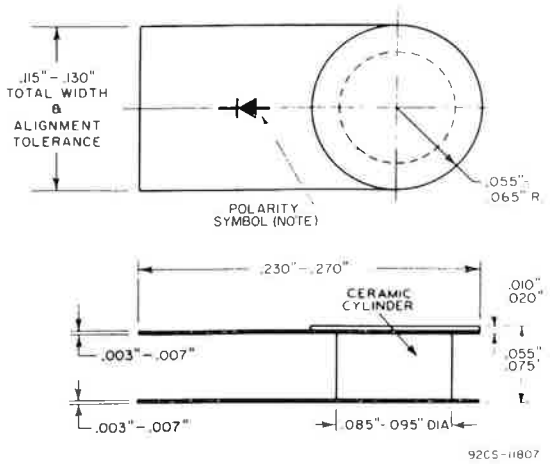

92CS-11807

NOTE: ARROW INDICATES DIRECTION OF FORWARD CURRENT FLOW AS INDICATED BY DC AMMETER.

Editor ..... **Bernard J. Simpson**

Radiotronics is published twelve times a year by the Wireless Press for Amalgamated Wireless Valve Co. Pty. Ltd. The annual subscription rate in Australasia is £1, in the U.S.A. and other dollar countries $3.00, and in all other countries 25/-.

Subscribers should promptly notify Radiotronics, P.O. Box 63, Rydalmere, N.S.W., and also the local Post Office of any change of address, allowing one month for the change to become effective.

Devices and arrangements shown or described herein may embody patents. Information is furnished without responsibility for its use and without prejudice to patent rights.

Information published herein concerning new releases is intended for information only, and present or future Australian availability is not implied.

Printed by CLOISTER PRESS (W. Short), REDFERN, N.S.W.